PERGAMON

Deep-Sea Research II 50 (2003) 833–851

DEEP-SEA RESEARCH
PART II

www.elsevier.com/locate/dsr2

Impacts of iron control on phytoplankton production in the modern and glacial Southern Ocean

Katja Fennel*, Mark R. Abbott, Yvette H. Spitz, James G. Richman, David M. Nelson

College of Oceanic and Atmospheric Sciences, Oregon State University, 104 Ocean Admin. Bld., Corvallis, OR 97331, USA

Accepted 5 October 2002

Abstract

Paleoceanographic evidence points to the Southern Ocean as a strong sink for atmospheric CO_2 during the Last Glacial Maximum (LGM), but no consensus about the responsible mechanism has yet been reached. Martin (Paleoceanography 5 (1990) 1) postulated that greater iron input during the LGM could have stimulated phytoplankton to consume the surface nutrients in the Southern Ocean, increasing carbon export substantially. We use a simple ecological model to elucidate the extent to which iron availability affects export production in the southwest Pacific sector. The model includes the effect of iron in a semi-explicit way. Based on the physiological response of the photosynthetic apparatus, the simulated phytoplankton growth rates are explicitly dependent on iron. The cycling of iron in the food web is not tracked, since uncertainties persist about the dynamics of iron uptake, transformation and release processes within the pelagic community. A simulation of the present ocean that uses the semi-explicit approach to include iron is compared with a simulation that accounts for iron only implicitly by using model parameters that are typical for low iron conditions. The simulations agree within the range of available observations. Glacial scenarios are simulated (assuming an increase in iron supply) and compared to the modern ocean simulation. Primary and export production increase in the glacial simulations, in particular if we assume an adaptation of the Si:N cell quota of diatoms to the higher iron levels. In this case the export doubles north of the Polar Front and in the Seasonal Ice Zone.

1. Introduction

Given the rise of atmospheric CO_2 levels and the prospect of global warming, understanding and predicting the ocean's role in global carbon cycling are probably the most pressing and challenging tasks in oceanography today. The oceanic carbon cycle is key to explaining large and geologically rapid changes on atmospheric CO_2 concentrations, since the reservoir of inorganic carbon in the ocean is about 60 times larger than in the atmosphere (Broecker, 1982). Any model prediction of future changes in oceanic carbon sequestration has to rely largely on practically untestable assumptions, leading to considerable uncertainty in model forecasts. To test our predictive capabilities, numerous studies have focused on explaining climate changes in the geological past, in particular during the Last Glacial Maximum (LGM)

*Corresponding author. Current address: IMCS, Rutgers University, New Brunswick, NJ 08901, USA. Tel.: +1-732-932-6555; fax: +1-732-932-8578.

E-mail address: kfennel@imcs.rutgers.edu (K. Fennel).

0967-0645/02/$ - see front matter
PII: S0967-0645(02)00596-9

($\sim$20,000 years ago; Bard et al., 1990). The LGM was characterized by substantially reduced atmospheric CO_2 concentrations (Monnin et al., 2001; Petit et al., 1999). A variety of paleoceanographic proxies allow a verification of suggested explanations for the change in atmospheric CO_2 and climate, at least to some degree.

Martin (1990) postulated that oceanic productivity in high nutrient, low chlorophyll (HNLC) regions such as the Southern Ocean is presently limited by iron deficiency and that this iron deficiency was relieved during glacial periods due to significantly increased aeolian iron deposition. Paleoceanographic proxies from ice cores (Petit et al., 1999, 1990) and sediment records (Kumar et al., 1995) indicate that dust deposition and iron fluxes to the sediments were higher during glacial periods. Martin (1990) further postulated that the increased iron supply enabled phytoplankton to consume nearly all of the upwelled nutrients in Southern Ocean surface waters, which presently persist at relatively high levels, and that the corresponding increase in carbon export could explain the low atmospheric CO_2 levels during that period. The idea of increased export production due to higher iron availability is supported by sediment records, which indicate higher fluxes of organic matter to the sediments during the LGM (Anderson et al., 1998; Kumar et al., 1995). Biogeochemical models suggest that a complete drawdown of Southern Ocean surface nutrients could affect the partitioning of carbon between the ocean and the atmosphere sufficiently to cause the lower atmospheric CO_2 levels observed during glacial periods (Popova et al., 2000; Sarmiento and Orr, 1991; Knox and McElroy, 1984). These model results represent an upper limit for the possible productivity increase during glacial periods.

In situ iron-enrichment experiments (Boyd et al., 2000; de Baar et al., 1995) and bottle incubations (Franck et al., 2000; Takeda, 1998; Scharek et al., 1997) consistently show an increase in primary production, phytoplankton biomass and nutrient uptake after iron addition in the Southern Ocean. Although all these results support the importance of iron in regulating primary productivity, they do not imply that iron is the ultimate control. An extrapolation from the local and short-time experiments to the scale of the ecosystem and geological time scales is problematic. In the Southern Ocean, it is plausible that other controls of productivity come into play if iron limitation is relieved and, so far, a complete drawdown of surface nutrients is not supported by observational evidence. None of the iron addition experiments showed a complete drawdown of macronutrients, but experimental artifacts cannot be excluded; bottle effects occur in incubation experiments and iron-enriched patches are diluted during in situ enrichments.

Most modeling studies point to a significantly increased carbon sink in the Southern Ocean during the LGM, but consensus about the responsible mechanism has not yet been reached. Theories involve either a strong increase in productivity in the Southern Ocean connected with increased export of carbon due to higher supply rates of iron (Popova et al., 2000; Lefèvre and Watson, 1999; Sarmiento and Orr, 1991; Martin, 1990; Knox and McElroy, 1984); changes in the ocean's alkalinity (Archer and Maier-Reimer, 1994); or a reduction of carbon exchange between the ocean and the atmosphere due to increased stratification or extended ice cover in the Southern Ocean with only moderately increased or even reduced levels of productivity (Elderfield and Rickaby, 2000; Sigman and Boyle, 2000; Stephens and Keeling, 2000; Toggweiler, 1999; Sarmiento et al., 1998; François et al., 1997).

To elucidate the extent to which iron availability affects the drawdown of nutrients and export production, we use a simple ecological model that includes the effect of iron on phytoplankton growth rates based on the known physiological response. Simulations of the modern and glacial Southern Ocean are performed. Applied to the modern Southern Ocean, the model captures important features of the biological system and resolves the biogeochemical differences between the regions north of the Polar Front (PF) and the Seasonal Ice Zone in good agreement with observations. To test how strongly the biologically mediated carbon export is controlled by the availability of iron, we perform simulations with increased iron supply, but leave the physical model component unaltered.

The paper is organized as follows. In Section 2 we briefly summarize some ecological and biogeochemical aspects of iron cycling in the ocean and introduce approaches to model the effect of iron in ecological models. Our model concept, set up and our parameterization of the effect of iron are described in Section 3 in Section 4 the simulated course of dissolved iron in the present ocean is compared with observations. The other biochemical variables are discussed in comparison to a model simulation that does not include iron explicitly (described in Fennel et al., 2003). In Section 5 we describe the simulations of glacial scenarios and discuss the results in relation to the modern ocean. A summary and conclusions are given in Section 6.

2. Iron regulation of phytoplankton growth

2.1. Regulation versus limitation—a remark

In the recent literature, iron is often described as limiting nutrient for phytoplankton growth in the Southern Ocean (usually in reference to iron-enrichment experiments) without clearly defining limitation. This is imprecise and unfortunate, in particular since Cullen (1991) pointed out early in the debate about the importance of iron that precision is essential when discussing hypotheses. To describe limitation, two concepts are common. According to Liebig (1855), the limiting nutrient is the one that determines total crop yield, or in other words, is the nutrient in shortest supply relative to need. In contrast, a factor is rate-limiting if it depresses the actual growth rate.

Iron-enrichment experiments test if phytoplankton growth is rate-limited by iron availability. In the oceanic environment, the phytoplankton growth rate, however, is rarely limited by only one factor. Although one factor might have a profound influence on primary productivity and ultimate nutrient utilization, the interaction of many factors determines how the system works (Cullen, 1991). For the Southern Ocean it has been pointed out that light and grazing are important controls of the phytoplankton growth rate besides iron (Mitchell et al., 1991; Nelson and Smith, 1991; Frost, 1991), and it is not clear which factor ultimately determines primary and export production.

In this paper we attempt to be specific and avoid the term "iron limitation". Instead, we will consider iron or any other factor as regulation of phytoplankton growth if its variation changes the phytoplankton growth rate. For example, for a Michaelis–Menten type response of the growth rate, regulation occurs in the linear slope area of the parameterization.

2.2. Ecological aspects of iron cycling

The micronutrient iron is essential for phytoplankton growth and is found primarily in the catalytic centers of enzymes. These iron-containing proteins play an important role in photosynthetic and respiratory electron transfer processes and are directly involved in nitrate reduction and chlorophyll synthesis (Raven, 1988). The most notable symptom of iron deficiency in phytoplankton is a reduction in photosynthetic pigment content, also termed chlorosis, and a decrease in photosynthetic efficiency (Geider and La Roche, 1994; Greene et al., 1991, 1992). Greene et al. (1991) describe the physiological responses of the photosynthetical apparatus to iron deficiency in a marine diatom. They found a decrease in Chl:C ratios and a decrease in chl-specific light-saturated photosynthesis P^{B}_{max}, resulting mainly from a reduction of the photosystem II reaction center protein, and suggest an increase of the fraction of non-functional reaction centers under iron-depleted conditions.

The cycling of iron in the ocean is comparable to the dynamics of macronutrients in some vital respects. Profiles of dissolved iron concentrations are similar to the distribution of nitrogen and phosphorus (Johnson et al., 1997). Concentrations are low at the surface due to depletion by biological uptake and increase with depth due to remineralization in the subsurface and deep ocean. Also the recycling of iron within the pelagic food web displays similarities to that of macronutrients, with excretion of dissolved forms of iron by grazers and rapid utilization of this recycled iron by phytoplankton (Hutchins et al., 1995, 1993).

There are important qualitative differences in biogeochemical cycling of iron compared to nitrogen, phosphorus and silica. The major fraction of dissolved iron in surface waters is bound to organic ligands that apparently increase iron availability (Rue and Bruland, 1995; Wu and Luther, 1995; Gledhill and van den Berg, 1995). Different phytoplankton groups use different mechanisms to access the organically bound iron (Hutchins et al., 1999), but the nature of this uptake is not yet well known. Photochemical reduction of colloidal iron has been suggested as another important process to make iron bioavailable (Barbeau et al., 2001). It is thought that the concentration of dissolved organic matter sets an upper limit for the dissolved iron concentrations, while free iron is scavenged and quickly removed from the system (Johnson et al., 1997; Sunda, 1997). Hence there appears to be a true interaction between dissolved iron and biota where the biota determine the availability of iron through the production of iron-binding ligands and the growth of biota in turn is determined by iron availability (Geider, 1999; Sunda, 1997).

Furthermore, the Fe:C ratio of phytoplankton is extremely flexible compared to the relatively constant elemental composition in macronutrients. Sunda and Huntsman (1995) found variations in intracellular Fe:C ratios of one order of magnitude for cultures of oceanic diatoms at different ambient iron concentrations. Also Fe:C ratios determined from the slope of dissolved iron concentration versus apparent oxygen utilization (AOU) for different oceanic regions vary for different ambient iron concentrations. Small Fe:C ratios of ~ 2 μmol:mol are estimated in the HNLC regions equatorial Pacific and Southern Ocean (consistent with the observation that iron availability is low in these regions), while values between 7 and 13 μmol:mol are found for the North Atlantic (Sunda, 1997).

During the last decade, much progress has been made in understanding biogeochemical and physiological aspects of iron cycling in the ocean, but many components are still poorly understood. Uncertainties persist about the supply rates of iron from the atmosphere and the deep ocean (Fung et al., 2000), the chemical speciation of iron, and which of the chemical species are biologically available (Measures and Vink, 2001; Wells et al., 1995). Also, the dynamics of iron uptake, transformation and release processes within the pelagic community are still poorly constrained (Hutchins et al., 1999; Geider, 1999; Schmidt et al., 1999).

2.3. Concepts of including iron in ecological models

Models that include an effect of iron availability on biogeochemistry have been developed by Moore et al. (2002a,b) for a global domain; by Christian et al. (2002a,b); Chai et al. (2000); Leonard et al. (1999) and Loukos et al. (1997) for the equatorial Pacific; by Denman and Peña (1999) for the subarctic Pacific; and by Hense et al. (2000) and Lancelot et al. (2000) for the Southern Ocean. There are two general approaches to model the biological effect of iron, although the details of the actual parameterization vary in these models. In the first approach (Chai et al., 2000; Hense et al., 2000; Denman and Peña, 1999) the phytoplankton growth parameters are changed as a proxy for iron regulation, while no explicit iron response is included. In this case the iron dynamics within the biological system and the supply rates of iron are ignored. This approach can be seen as a sensitivity test of the model to variations in phytoplankton growth parameters.

The other general approach (Christian et al., 2002a,b; Lancelot et al., 2000; Moore et al., 2002a,b; Leonard et al., 1999) includes iron explicitly as a state variable and tracks the cycling of iron through the biological system similar to nitrogen and other macronutrients. In these models, a Michaelis–Menten uptake response is used to determine the effect of iron availability on the growth rate. The rate-limiting nutrient is chosen as the one in shortest supply relative to need. The similar treatment of iron and nitrogen in these models implies a tight coupling between the elemental cycles of these nutrients.

3. The model

The physical/biological model used in this study is based on the description in Fennel et al. (2003).

The biological model component contains eight state variables: two phytoplankton groups, diatoms *dia* and other small phytoplankton *phy*; one group of zooplankton *zoo*; three inorganic nutrient pools, dissolved inorganic nitrogen *din*, silicic acid *sia* and dissolved iron *fe*; and two detrital pools, detrital nitrogen det_N and detrital silicate det_{Si}. The elemental cycles of nitrogen and silica are included, while the elemental cycling of iron is not fully tracked. Diatoms are treated as a separate phytoplankton group and the "silica pump", an efficient mechanism for the removal of silica from the euphotic zone (Dugdale et al., 1995), is resolved by considering the detrital fractions of nitrogen and silica as separate pools. The phytoplankton growth parameterizations include a physiologically based response to changes in iron supply (described in Section 3). The zooplankton group represents microzooplankton that grazes only on the small phytoplankton and provides "top-down" control on the small phytoplankton—an important feature of the biological system in that region.

This model is coupled to a one-dimensional physical model and applied to three stations in the southwest Pacific sector of the Southern Ocean, along 170°W. One model station at 56°S lies north of the PF, one station at 61°S is located in the vicinity of the PF, and the southernmost station at 64°S represents the Seasonal Ice Zone (SIZ). The physical model component simulates the vertical mixing of the state variables and the evolution of the mixed-layer depth in response to surface fluxes of heat and momentum following the parameterization of Price et al. (1986). The model is set up on a uniform grid covering the upper 400 m of the water column with a 5 m resolution and forced with daily values of wind stress and surface heat fluxes from the NCEP re-analysis data set. A detailed description is given in Fennel et al. (2003).

From our present knowledge of iron chemistry in seawater and the availability of iron to phytoplankton, it is evident that the elemental cycling of iron is intricate and qualitatively different from the cycling of macronutrients. Microbial activity modifies ocean chemistry by producing iron-binding ligands, and the organically bound iron in turn affects the ability of the ocean to support the microbial community (Geider, 1999; Sunda, 1997; Wells et al., 1995). The remineralization of iron and nitrogen in the food web is qualitatively similar, but appears to be a differential process (Hutchins et al., 1993). Macronutrients can be represented in a plausible way in biogeochemical models that neglect dissolved organic matter, but microbial physiology and the dynamics of dissolved organic matter seem to be key to understanding the cycling of iron (Geider, 1999).

Given this, we refrain from including the full cycle of iron in the biological system. Our approach is intermediate between the two presently common ways to model iron (described in Section 2.3). We represent the effect of iron based on the observed physiological response as a modulation of the phytoplankton growth rate, which goes beyond the use of a low phytoplankton growth rate as a proxy for iron-stress. The cycling of iron within the food web is included in a semi-explicit way in our model, where iron is taken up proportionally to the uptake of nitrogen, but not tracked further through the biological system. Instead, a weak restoration to the iron initial concentration provides a continuous resupply during the growing period, qualitatively representing the recycling within the food web, and replenishes iron during the non-growing period. This treatment of iron is combined with an ecological model that was developed for the southwest Pacific sector of the Southern Ocean (Fennel et al., 2003). In Fennel et al. (2003), iron is taken into account implicitly by choosing typical growth parameters and a typical Si:N stoichiometry for the diatoms. Here we include an explicit iron control of phytoplankton growth, based on the known physiological response of phytoplankton to iron deficiency.

In Fennel et al. (2003) we employed the following parameterization for the growth rate of diatoms

$$\mu_{dia}(E, sia, din) = \mu_{dia}^{max}(1 - \exp(-\bar{\alpha}E)) \times \min\left(\frac{sia}{k_{Si} + sia}, \frac{din}{k_N + din}\right). \quad (1)$$

The response of the growth rate to the inorganic nutrient concentrations is assumed to follow Michaelis–Menten kinetics while the nutrient in shortest supply is actually regulating the growth rate. The light dependence of photosynthesis is based on the P versus E curve given in Cullen (1990).

Here we modify the parameterization (1) to include the main physiological response of phytoplankton to iron deficiency, that is, the reduction of the efficiency of their photosynthetic apparatus (Geider and La Roche, 1994; Greene et al., 1991, 1992). Greene et al. (1991) report a 3-fold decrease in Chl:C ratios, a 2-fold reduction of the chl-specific light-saturated photosynthesis P^{B}_{max}, and a 1.3-fold increase in the chl-specific initial slope of the PE-curve α^{B} between iron-replete and iron-deficient diatom cells. The slight increase in α^{B} can be attributed to the overall reduction of light-harvesting pigments which reduces the "package" effect (Greene et al., 1991; Berner et al., 1989) and is ignored for our purpose. Since our model considers biomass in units of nitrogen and does not track a dynamic Chl:C ratio, we have to translate the chl-specific effects reported by Greene et al. (1991) into nitrogen units of biomass. The chl-specific P^{B}_{max} is implicitly contained in the biomass-specific maximum growth rate μ^{max}_{dia} and in the light parameter $\bar{\alpha}$, which corresponds to the ratio of α^{B} and P^{B}_{max}. We assume that an iron-dependent P^{B}_{max} should qualitatively show a Michaelis–Menten type response, with a slope range, where the photosynthetic efficiency increases proportional with iron supply, and a saturation region. These assumptions yield

$$\mu_{dia}(E, sia, din, fe) = \mu^{max}_{dia} \frac{fe}{k_{Fe} + fe} \left(1 - \exp\left(-\frac{\bar{\alpha} E}{fe}(k_{Fe} + fe)\right)\right) \cdots \min\left(\frac{sia}{k_{Si} + sia}, \frac{din}{k_{N} + din}\right). \quad (2)$$

The new parameter k_{Fe} represents a half-saturation concentration for iron and is set to 0.2 μmol m^{-3}. This value was estimated by Price et al. (1994) for the subtropical Pacific and is used in the models of Moore et al. (2002a,b) and Lefèvre and Watson (1999). The parameters μ^{max}_{dia} and $\bar{\alpha}$ need to be redefined in (2) for formulations (1) and (2) to be consistent. We define the two parameters such that the parameterization (2) yields the same rates as (1) for typical iron concentrations in the present southwest Pacific sector of the Southern Ocean. For an average iron concentration of 0.15 μmol m^{-3} during the AESOPS cruises (Measures and Vink, 2001) and $k_{Fe} = 0.2$ μmol m^{-3} this constraint yields $\mu^{max}_{dia} = 1.63$ d^{-1} and $\bar{\alpha} = 0.13$ $(W m^{-2})^{-1}$. These parameter choices imply that for an increased iron concentration during glacial periods, e.g. 2.5 μmol m^{-3}, the growth rate would double. A doubling of the growth rate is a reasonable assumption (Popova et al., 2000; Banse, 1991,1996) and is in agreement with the results of incubation experiments performed during the AESOPS study by Valerie Franck (personal communication), who found a doubling of the silica uptake rates after addition of 2.5 μmol Fe m^{-3}.

4. Simulating the present ocean

We performed a simulation for the period of the AESOPS field study. In this section we discuss the simulated iron distributions in comparison with iron concentrations measured during AESOPS. We also compare the simulated behavior of the other biochemical variables to the simulation that does not include iron explicitly (discussed in detail in Fennel et al., 2003).

4.1. Cycling of iron in the water column

In the contemporary Southern Ocean, deep mixing during winter and upwelling of iron-rich sub-surface waters are the main sources of dissolved iron in surface water. Aeolian deposition plays only a minor role (Fung et al., 2000; Lefèvre and Watson, 1999). Locally, significant amounts of iron can be added during ice melt, e.g., in the Ross Sea (Sedwick and DiTullio, 1997; Sedwick et al., 1996), but in the southwest Pacific sector this input is negligible (Measures and Vink, 2001). Observed concentrations of dissolved iron in the southwest Pacific sector of the Southern Ocean are

generally below 0.5 μmol m^{-3}. Within the small range of 0–0.5 μmol m^{-3}, the values exhibit strong spatial and temporal variations, mainly attributed to the high physical variability in the region (Measures and Vink, 2001).

Unfortunately, dissolved inorganic iron concentrations depend on the analytical approach used for its determination. This adds to the persisting uncertainty about which chemical forms of iron are present in seawater and which are biologically available. During the AESOPS study, values determined by shipboard flow injection analysis as described in Measures et al. (1995) were significantly higher in the upper 300–400 m of the water column than the values in replicate samples determined by atomic absorption spectrophotometry after preconcentration by chelation-solvent extraction after Johnson et al. (1997). Below 400 m water depth, the values agree well for both methods. The differences are attributed to different sensitivities of the methods to the organic fractions of iron (Measures and Vink, 2001). We base our data comparisons on the values determined by Measures and co-workers, since their values probably include a portion of organically complexed iron that is potentially available to phytoplankton but not determined by the solvent extraction method.

During AESOPS the surface concentrations of dissolved iron range between 0.075 and 0.34 μmol m^{-3} (Measures and Vink, 2001), in agreement with other measurements in open waters of the Pacific sector (Sedwick et al., 1997; de Baar et al., 1999). Variations in dissolved iron concentrations are most pronounced in the vicinity of the PF, where the highest average mixed layer concentrations of iron are found and the strongest seasonal depletion occurs (Measures and Vink, 2001). Iron concentrations below 200 m depth are stable between 0.25 and 0.3 μmol m^{-3}. The surface concentrations decrease over the course of the growing season due to biological uptake and the lowest values are reached in late summer. Pre-season values display a north to south gradient, with concentrations increasing from $\sim$0.2 μmol m^{-3} in the PFZ to $\sim$0.35 μmol m^{-3} in the SIZ. In summer this general pattern is reversed with surface concentrations decreasing from 0.2 to 0.3 μmol m^{-3} in the PFZ to $<$0.15 μmol m^{-3} in the Ross Sea. The PF is an exception and displays the widest range of values from $<$0.15 to $>$0.3 μmol m^{-3}.

The initial iron concentrations for the model simulation are set to 0.25 μmol m^{-3}, 0.3 μmol m^{-3} and 0.35 μmol m^{-3} for the stations at 56°, 61° and 64°S, respectively. These values are pre-spring estimates and based on maximum dissolved iron concentrations found at 250 m depth. Iron is taken up proportionally to the uptake of nitrogen by diatoms and small phytoplankton, and is resupplied by a weak restoration of the iron concentrations to the initial conditions. A comparison of the simulated iron profiles with the available iron data is shown in Figs. 1–3. At 61°S the simulated concentrations below 150 m water depth remain stable at the initial concentration of 0.3 μmol m^{-3} (Fig. 1). Surface concentrations are reduced by biological uptake to a minimum of 0.18 μmol m^{-3} in mid December at this station. The corresponding data vary, but the simulated and observed magnitudes and the seasonal decrease in surface concentrations agree. Fewer data profiles are available for the northern station at 56°S, but the simulated and observed values in February/March agree (Fig. 2). At 64°S the strongest iron depletion occurs (Fig. 3). The subsurface concentrations of 0.35 μmol m^{-3} are higher than at the other stations and the minimum concentration of 0.13 μmol m^{-3} occurs in mid-January. The resupply of iron by restoring its concentration weakly to the initial values yields inputs of $\sim$0.001 μmol Fe m^{-3} d^{-1} during the growing season at all stations. A maximum restoration flux of 0.002 μmol Fe m^{-3} d^{-1} occurs at station 64°S during January.

4.2. The other biochemical variables

The simulated course of the other biochemical variables is very similar to the simulation without explicit inclusion of iron. A detailed data comparison of the model results without explicit iron is given in Fennel et al. (2003) and shows that essential features of the biological system in the PFZ, in the vicinity of the PF, and in the SIZ are captured, including the seasonal patterns of

dissolved inorganic nitrogen and silicic acid, biogenic silica, primary production, and vertical particle flux.

A notable difference between the two simulations is found only for the variables that are connected with the silica cycle, namely silicic acid and diatoms. The results for dissolved inorganic nitrogen, small phytoplankton and zooplankton do not change noticeably. A comparison of the simulated course of silicic acid and biogenic silica in both simulations is shown in Fig. 4. The major difference is a time shift in the drawdown of silicic acid and correspondingly in the maximum of biogenic silica, which occurs earlier in the current simulation. The maximum concentrations of biogenic silica are higher than in the version without explicit iron (by up to 5 mmol Si m^{-3} at 64°S), but the changes lie within the range of the observed values. Also, the simulated annual primary productivity and the vertical export flux increase slightly, but lie within the uncertainty of the data.

The agreement between the two model versions shows that the inclusion of iron has been done consistently with the former version and supports

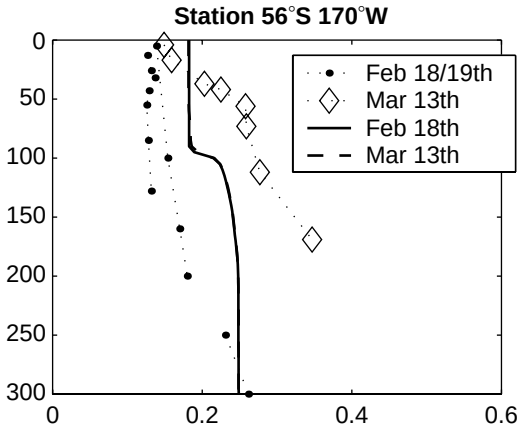

Fig. 2. Simulated (solid and dashed lines) and observed (diamonds and filled dots) dissolved iron concentrations at 56°S.

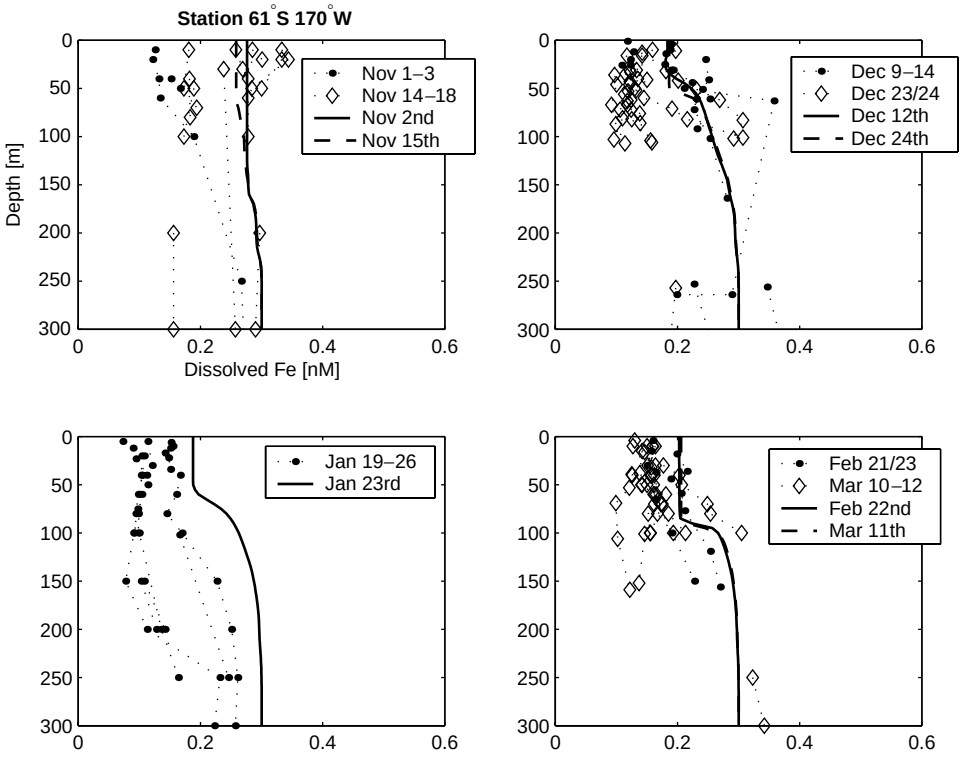

Fig. 1. Simulated (solid and dashed lines) and observed (diamonds and filled dots) dissolved iron concentrations at 61°S. The dissolved iron measurements by Christopher Measures and co-workers are used.

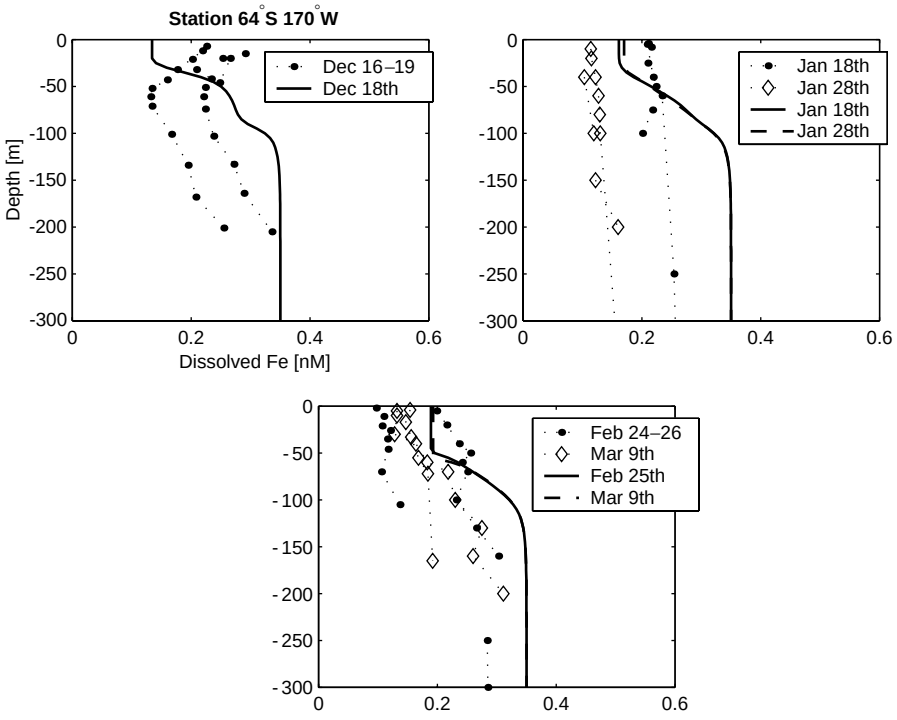

Fig. 3. Simulated (solid and dashed lines) and observed (diamonds and filled dots) dissolved iron concentrations at 64°S.

the idea that an implicit treatment of the iron effect can describe the present situation in the Southern Ocean reasonably within the range of variation in the observations.

5. Glacial scenarios

5.1. Motivation and assumptions

During the LGM, the physical and biochemical environment in the Southern Ocean was different than today. Differences in physical features include increased wind speeds, colder sea-surface and atmospheric temperatures, greatly expanded winter sea-ice cover, increased stratification due to increased meltwater input and increased deposition of atmospheric dust (Moore et al., 2000). Uncertainty persists about the consequences of these changes for the carbon cycle and which feature in particular is important for the lowered atmospheric CO_2 levels during the LGM ($\sim$80 ppm lower than pre-industrial levels of $\sim$280 ppm). In the ongoing debate, explanations range from purely physically induced changes, due to increased ice cover along with reduced productivity, to theories that suggest a significant contribution from biologically induced carbon export (Stephens and Keeling, 2000; Elderfield and Rickaby, 2000; Sigman and Boyle, 2000; Moore et al., 2000; Popova et al., 2000; Lefèvre and Watson, 1999). An earlier model study has shown that the biological export to be expected for a complete drawdown of surface phosphate could theoretically cause the glacial drawdown of CO_2 (Sarmiento and Orr, 1991), but more realistic assumptions about the productivity increase in recent box model studies indicate a smaller effect of the biology in response to the higher iron supply between 10 and 30 ppm (Popova et al., 2000; Lefèvre and Watson, 1999).

To investigate the role of iron in changing primary and export production, we apply our

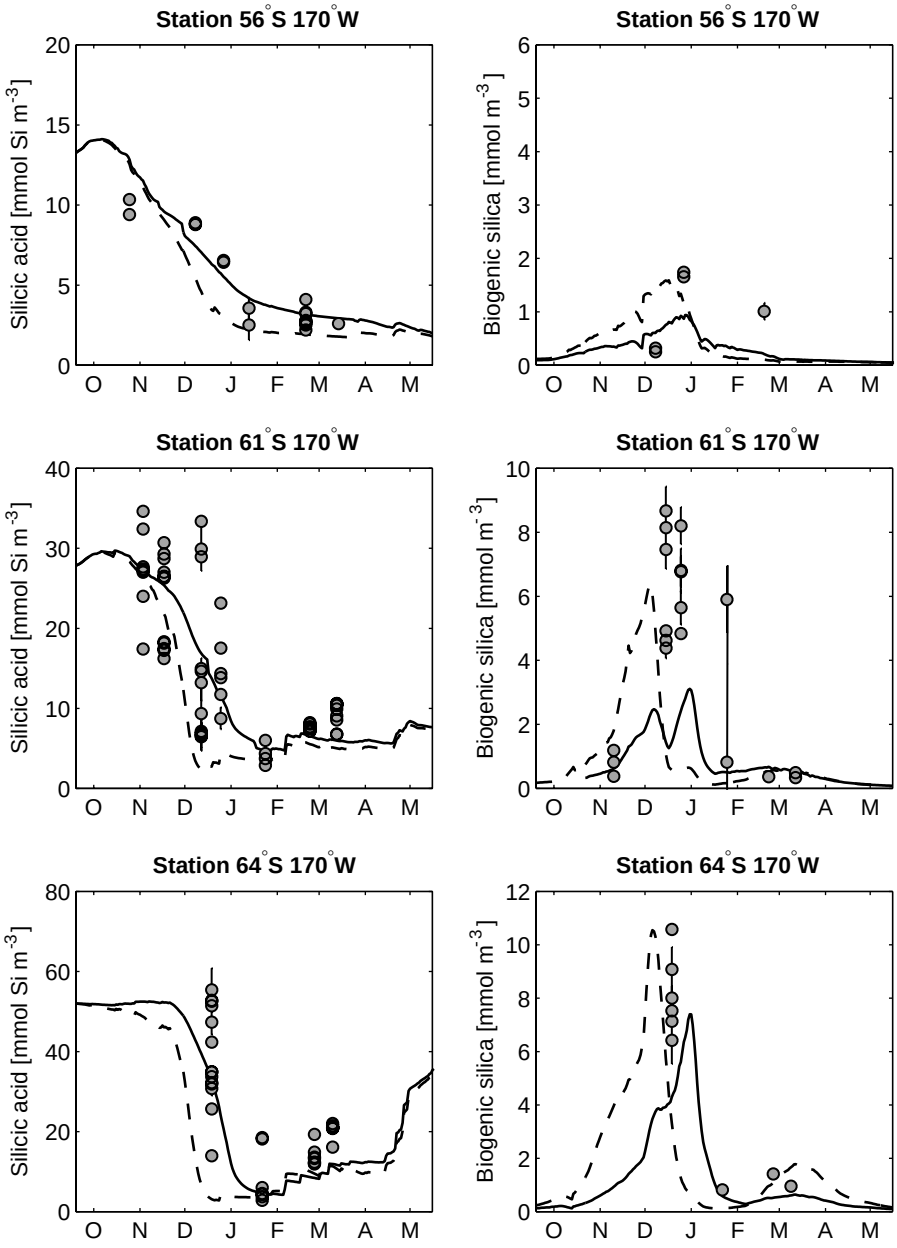

Fig. 4. Simulated course of surface silicic acid and biogenic silica in the current model version (dashed line) in comparison to the simulation without explicit iron in Fennel et al. (2003) (solid line) at three stations along 170°W. The filled circles represent surface values measured during the AESOPS field study (Brzezinski et al., 2001).

ecological model, which includes the major controls of the present biological system in the Southern Ocean, to glacial iron conditions. Our glacial scenario is unrealistic with respect to the physical conditions, which we do not alter, since colder temperatures and increased stratification may have had ecological consequences. Furthermore, we assume no substantial changes in the

supply of the macronutrients nor in the ecological structure of the system.

5.2. Simulations

We performed three simulations of glacial scenarios. Since iron supply by atmospheric dust deposition was higher during glacial periods—sediment and ice-core records suggest an increase by a factor of 15–50 (Petit et al., 1999; Kumar et al., 1995)—we have increased the initial iron concentration by an order of magnitude to 3 μmol m^{-3} in these simulations. This is an optimistic assumption considering that modern concentrations of dissolved iron in the deep ocean are about 0.6 μmol m^{-3} (Johnson et al., 1997).

In the first glacial simulation we do not adjust the functioning of the ecosystem and employ the same parameter set as for the modern ocean. It is, however, reasonable to assume some adaptation of phytoplankton to the increased iron levels; in particular the Si:N ratio of the diatoms and the Fe:C ratio of both phytoplankton groups were probably different.

In the second and third glacial scenario we expore how changes in the Si:N and Fe:C ratios affect the system. The Si:N ratio of 4 in our modern simulation is reduced to 2 in the second and third glacial simulation. The heavy silicification of the diatoms and the high Si:N disappearance ratios observed in the contemporary Southern Ocean are thought to be due to iron stress. Cultured diatoms increase their Si:N stoichiometry by a factor of 2 to 3 under iron-depleted conditions (Takeda, 1998; Hutchins and Bruland, 1998).

In the third scenario, we also adjust the Fe:C ratio of both phytoplankton groups. While the C:N:P ratio of marine phytoplankton is relatively constant (Redfield et al., 1963), the Fe:C ratio is known to be flexible and adapts to the ambient iron levels (Sunda, 1997). Sunda and Huntsman (1995) showed that the cellular Fe:C ratio in cultured oceanic diatoms varies from 2.5 to 34 μmol:mol for different iron concentrations. Fe:C ratios of particulate organic matter, estimated from profiles of dissolved iron concentration and apparent oxygen utilization (AOU), range between 7 and 13 μmol:mol for the North Atlantic and ~2 in the Southern Ocean and equatorial Pacific, both characterized by low iron levels (Sunda, 1997). To explore the effect of a different Fe:C stoichiometry, we increased the Fe:C ratio for both phytoplankton groups from 2 μmol:mol in the previous simulations to 5 μmol:mol in the third simulation (based on Johnson et al., 1997).

In the second and third simulations—both run with the same Si:N ratio of 2 and differing only in their Fe:C stoichiometry—the course of the macronutrients and of the plankton variables does not change noticeably. The surface iron concentrations differ slightly; minimum surface iron concentrations are about 0.1 μmol m^{-3} lower for a Fe:C ratio of 5 than for a Fe:C ratio of 2. These slight variations in iron concentrations do not affect the phytoplankton growth rates or the other biochemical variables. We therefore restrict the following comparison to the simulations of the modern ocean and the two glacial scenarios that only differ in the Si:N stoichiometry of the diatoms.

The simulated course of the surface macronutrients in the present ocean is shown in comparison with the glacial scenarios in Fig. 5. The drawdown of dissolved inorganic nitrogen is stronger in the glacial simulations compared to the present ocean and is more pronounced if we assume adaptation of the Si:N ratio of the diatoms. Also the uptake of silicic acid is stronger in the glacial simulations, but more pronounced in the simulation which assumes the higher Si:N stoichiometry (representing heavily silicified diatoms). At 61°S and 64°S, silicic acid is depleted in both glacial simulations, while the magnitude of nitrogen consumption at these stations is strongly affected by the different assumptions about the Si:N stoichiometry.

At 56°S the drawdown of inorganic nutrients increases in the glacial simulations, but the nutrients are not depleted completely and the drawdown is slow. This implies that the light/mixing regime plays an important role in controlling productivity in all simulations at this station. At 61°S and 64°S, silicic acid ultimately limits phytoplankton production. The magnitude of the seasonal silicic acid consumption is determined by

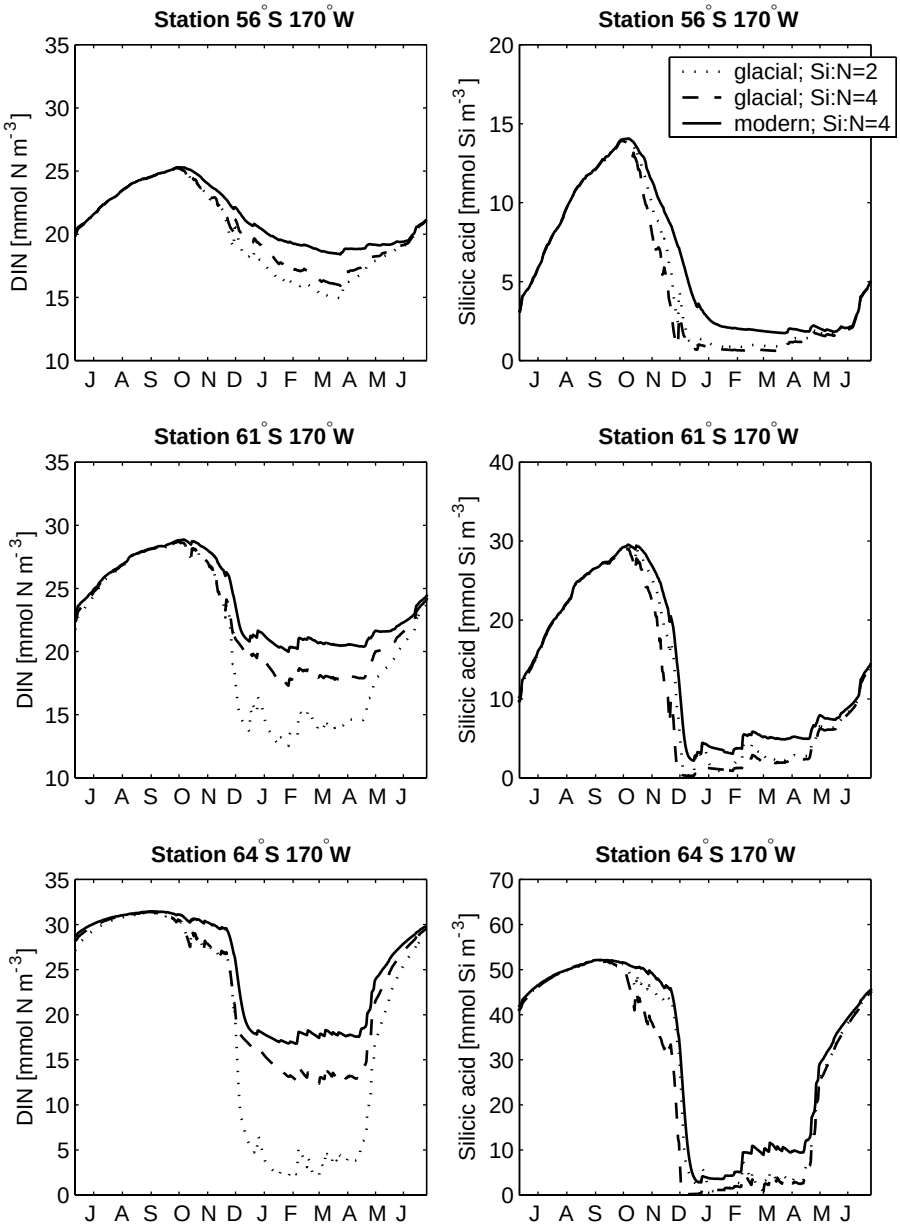

Fig. 5. Simulated course of surface nutrients for the simulation of the modern ocean and the two glacial scenarios that assume the same Fe:C ratio.

the pre-season concentration. Dissolved inorganic nitrogen is always replete.

The simulated diatom biomass is higher in the glacial scenarios than in the modern ocean (Fig. 6). The highest standing stocks are reached if the Si:N stoichiometry is assumed to adapt. At 61°S and 64°S, the maximum diatom biomass is 2.2 and 4.3 mmol N m^{-3} for the modified Si:N ratio, that is about twice the maximum concentrations of 1.0 and 2.0 mmol N m^{-3} if diatoms use the surface

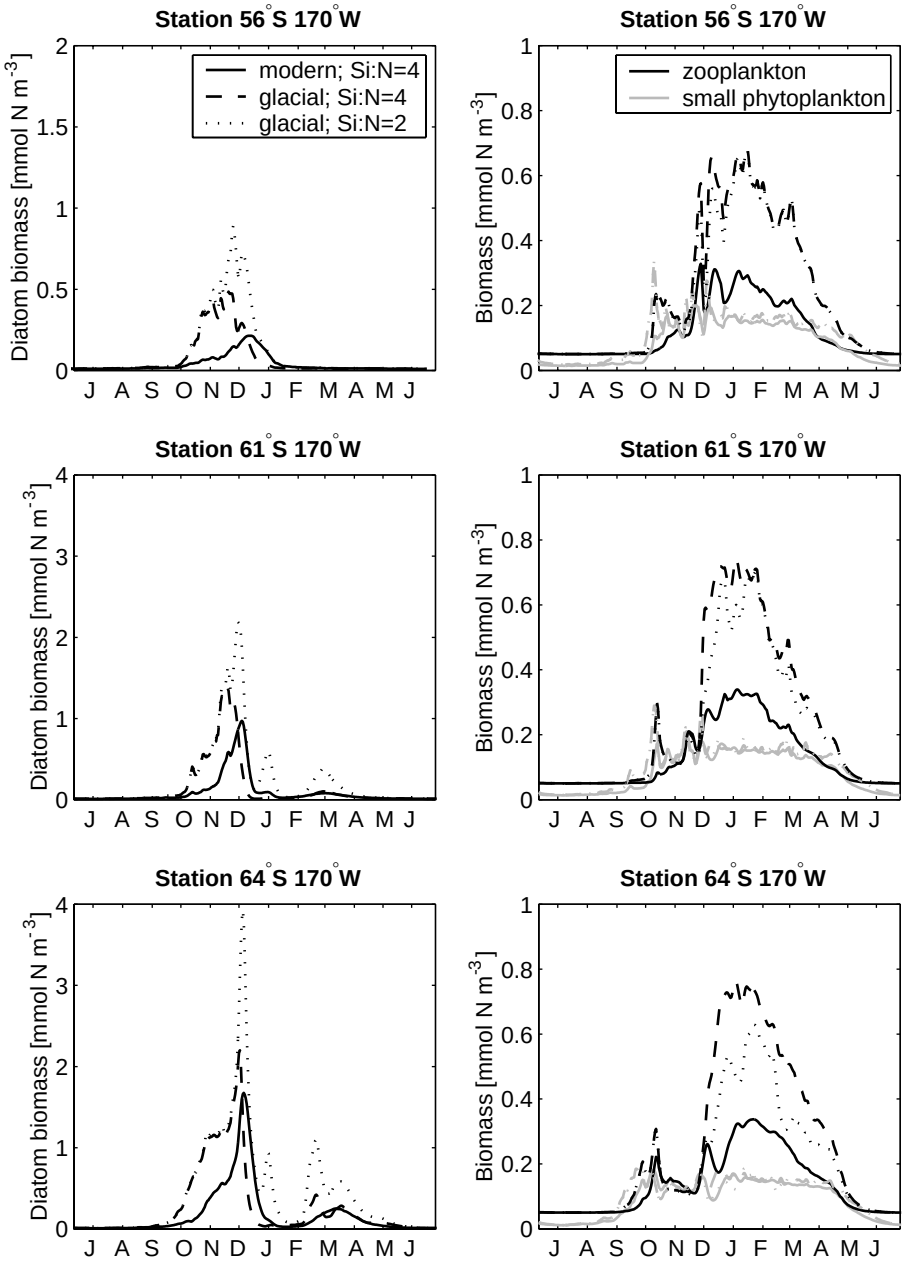

Fig. 6. Simulated course of diatom biomass (left panels) and biomass of the small phytoplankton (right panels; gray lines) and the zooplankton (right panels; black lines) for the simulation of the modern ocean and the two glacial scenarios.

silica less efficiently in the case without adaptation. At the southernmost station, the maximum diatom biomass does not change significantly between the modern and glacial scenario if the same Si:N ratio is used. The indirect effect of the increased iron levels (reduction of the Si:N stoichiometry of diatoms) is larger than the direct effect on the growth rate.

The biomass of small phytoplankton does not change in the glacial scenarios compared to the modern ocean, but standing stocks of their zooplankton grazers are higher. Zooplankton are grazing efficiently on the small phytoplankton, hence an increase of the phytoplankton growth rate is reflected in higher zooplankton biomass while small phytoplankton do not accumulate at higher levels.

The daily vertical particle fluxes of detrital silica and detrital nitrogen at 400 m depth are compared in Fig. 7. A considerable increase in the glacial

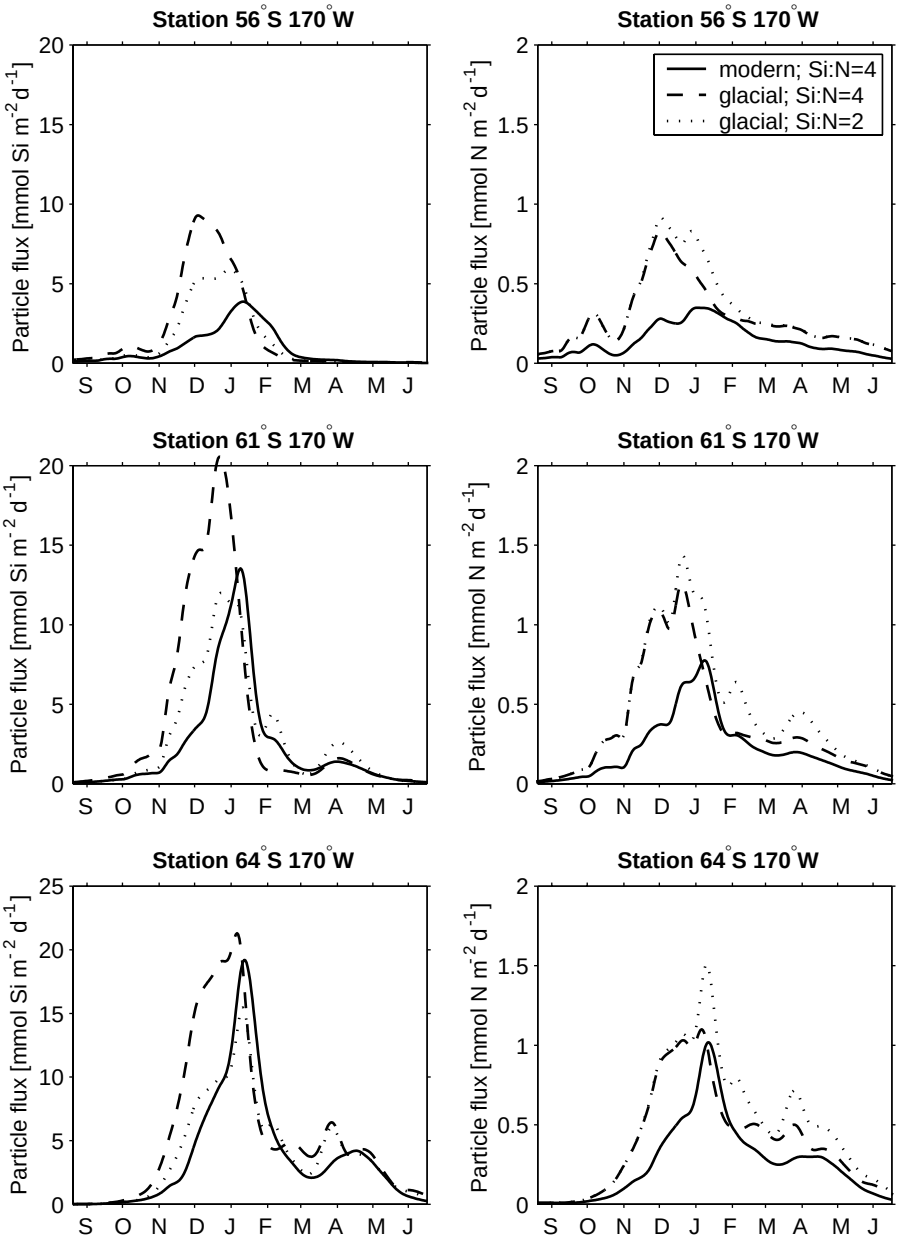

Fig. 7. Simulated vertical particle fluxes at 400 m depth for the simulation of the modern ocean and the two glacial scenarios.

silica fluxes is found only at 56° and 61°S. At 64°S the fluxes do not increase significantly if the Si:N ratio of the diatoms is reduced. The vertical fluxes of detrital nitrogen, which are representative for the vertical flux of biogenic carbon (if we assume a constant C:N stoichiometry) increase at all stations in both glacial simulations. Higher vertical nitrogen flux occurs for a reduced Si:N ratio of the diatoms, further supporting the idea that a change in the Si:N stoichiometry of the diatoms allows a more efficient export of nitrogen relative to silicate export.

The annual vertical particle fluxes and the annual uptake of dissolved inorganic nitrogen and silicic acid for the modern and the two glacial simulations are given in Table 1. In the glacial simulation that uses the reduced Si:N cell quota for diatoms the yearly total uptake of dissolved inorganic nitrogen and silicic acid roughly doubles at all stations compared to the modern ocean. The vertical fluxes of particulate nitrogen and silica increase everywhere in the glacial simulations relative to the modern ocean.

Table 1
Simulated vertical particle fluxes at 400 m and total uptake of dissolved inorganic nitrogen and silica in the euphotic zone

	56°S 170°W	61°S 170°W	64°S 170°W
Total DIN uptake (mol N m^{-2} $year^{-1}$)			
Modern	1.2	1.7	2.1
Glacial; Si : N = 4	2.3	2.9	3.3
Glacial; Si : N = 2	2.6	3.4	4.0
Total Si uptake (mol Si m^{-2} $year^{-1}$)			
Modern	0.30	0.80	1.39
Glacial; Si : N = 4	0.64	1.32	2.10
Glacial; Si : N = 2	0.97	2.08	3.07
Simulated flux of det_{Si} (mol Si m^{-2} $year^{-1}$)			
Modern	0.27	0.70	1.16
Glacial; Si : N = 4	0.58	1.15	1.72
Glacial; Si : N = 2	0.41	0.86	1.21
Simulated flux of det_N (mol N m^{-2} $year^{-1}$)			
Modern	0.05	0.07	0.08
Glacial; Si : N = 4	0.09	0.11	0.12
Glacial; Si : N = 2	0.10	0.14	0.15
Si:N ratio of simulated vertical flux (*mol:mol*)			
Modern	6.06	10.65	14.31
Glacial; Si : N = 4	6.43	10.22	14.36
Glacial; Si : N = 2	4.09	6.30	8.27

6. Summary and conclusions

A simple ecological model was used to simulate the biological system in the Pacific sector of the Southern Ocean for modern and glacial iron supply conditions. The model includes the physiological response of phytoplankton to the dissolved iron availability, namely a decrease in the maximum photosynthetic efficiency under iron deficiency, but does not track the cycling of iron through the food web. Given the present understanding of the elemental cycle of iron and the existing uncertainties, it appears premature to attempt an explicit model of the cycling of iron in the biological system. Simplified concepts based on the qualitative effects of iron on phytoplankton growth, which are used in different recent modeling studies (see Section 2.3) and in this study, seem, however, appropriate to investigate questions about the effect of iron on biological carbon export.

We performed a simulation for the present ocean. A comparison of the simulated iron concentrations with observations showed good agreement in magnitude and the seasonal course. We compared this simulation with a simulation of the present Southern Ocean that accounts for iron only implicitly by choosing typical parameters (discussed in Fennel et al., 2003). There was no significant difference between the two simulations within the given range of the observations, indicating that an implicit treatment of iron allows a reasonable description of the biological system in the present Southern Ocean within the range of available data.

Glacial scenarios were simulated, where the iron supply was increased but the physical environment was not altered. One simulation employs the same biological parameter set as the present ocean simulation. Additional simulations used a reduced Si:N cell quota for diatoms and an increased Fe:C uptake ratio for small phytoplankton and diatoms, accounting for an adaptation of phytoplankton to the higher iron levels. A modification of the Fe:C

ratio had no notable impact on the simulation results. Iron is at saturated levels in the glacial scenarios, hence a perturbation of the Fe:C uptake ratio has no effect. A change in Si:N stoichiometry of the diatoms has consequences for the export of carbon.

North of the PF, the annual phytoplankton production is strongly controlled by the available light. The concentration of silicic acid at the surface is reduced to levels where it regulates diatom production, but silicic acid is not completely depleted. In this situation the iron-induced increase in photosynthetic efficiency has a strong impact on carbon export almost doubling the annual vertical flux. The carbon export increases further if a reduction of the Si:N quota of the diatoms is included (the annual vertical flux doubles compared to the present ocean).

In the SIZ, silicic acid supply is a main control on annual phytoplankton production. Presently, the main productivity event is a short, intense diatom bloom that is observed to follow the retreating ice edge and depletes silicic acid concentrations at the surface (Brzezinski et al., 2001). In our model simulations, surface silicic acid is depleted in both glacial scenarios. If the amount of annually produced organic carbon, which can potentially be exported from the pelagic system, is constrained by the pre-spring level of silicic acid, no substantial increase in carbon export occurs if nutrients are taken up at a higher rate but with the same stoichiometric ratio. A reduction of the Si:N cell quota of the diatoms, which is a reasonable assumption, significantly increases the export of biogenic carbon (the annual vertical flux almost doubles compared to the present ocean).

Our results are consistent with the ideas of Moore et al. (2000) about the biological export during the LGM. North of the PF, they suggested higher biological carbon export as result of higher iron supply. For the seasonally ice-covered zone south of the PF the authors argued that productivity and carbon export would increase during the growing season due to higher iron inputs. During the rest of the year they suggested a reduced outgassing of CO_2 from the ocean because the extent of ice cover was probably increased and acted as a barrier to air–sea gas exchange. The results of our simulations suggest an additional increase of biological production in the Seasonal Ice Zone connected to a change in the diatom Si:N uptake quota.

The sediment record shows higher biological production in the Atlantic sector during the LGM compared to the present ocean and a northward shift of the high productivity region from its present position (Anderson et al., 1998; Kumar et al., 1995). Anderson et al. (1997) found a 5-fold greater accumulation of organic carbon during the LGM than today and a decoupling of the accumulation of biogenic silica and organic carbon. Consistent with our assumption of a reduced Si:N quota for diatoms a lower Si:C ratio was found during the LGM than today. Our simulations, assuming no changes in the physical environment and in the supply of macronutrients, show that an iron-induced stimulation of productivity can account for a 2-fold increase in organic carbon export. Changes in ice-cover, circulation, stratification, and nutrient upwelling would modify this estimate, in particular an increase in silicic acid availability would potentially increase carbon export.

Iron enrichment experiments in the Southern Ocean have consistently shown that nutrient uptake, chlorophyll concentration and phytoplankton biomass increase during iron enrichments. These results imply that iron is at regulating levels in the present Southern Ocean or, in other words, that iron is rate-limiting for phytoplankton growth. This does not necessarily imply an increase in carbon export for higher iron levels on an annual timescale. We have shown that the nutrient-uptake quota of diatoms and the supply of silicic acid are important in determining biological production and export on seasonal timescales.

Acknowledgements

We wish to thank Robert Anderson, Ekaterina Popova, Inga Hense and an anonymous reviewer for their thoughtful comments. This work has been supported by a grant from the National

Aeronautics and Space Administration (NAG5-4947). US JGOFS contribution no. 717.

References

Anderson, R.F., Kumar, N., Mortlock, R.A., Froelich, P.N., Kubik, P., Dittrich-Hannen, B., Suter, M., 1998. Late-quaternary changes in productivity of the Southern Ocean. Journal of Marine Systems 17, 497–514.

Archer, D., Maier-Reimer, E., 1994. Effect of the deep-sea sedimentary calcite preservation on atmospheric CO_2 concentration. Nature 367, 260–263.

Banse, K., 1991. Iron availability, nitrate uptake and exportable new production in the subarctic Pacific. Journal of Geophysical Research 96, 741–748.

Banse, K., 1996. Low seasonality of low concentrations of surface chlorophyll in the Subantarctic water ring: underwater irradiance, iron, or grazing? Progress in Oceanography 37, 241–291.

Barbeau, K., Rue, E.L., Bruland, K.W., Butler, A., 2001. Photochemical cycling of iron in the surface ocean mediated by microbial iron(III)-binding ligands. Nature 413, 409–413.

Bard, E., Hamelin, B., Fairbanks, R.G., Zindler, A., 1990. Calibration of ^{14}C timescales over the past 30,000 years using mass spectrometric U-Th ages from Barbados corals. Nature 345, 405–410.

Berner, T., Dubinsky, Z., Wyman, K., Falkowski, P.G., 1989. Photoadaptation and the "package" effect in *dunaliella tertiolecta* (Chlorophyceae). Journal of Phycology 25, 70–78.

Boyd, P.W., et al., 2000. A mesoscale phytoplankton bloom in the polar Southern Ocean stimulated by iron fertilization. Nature 407, 695–702.

Broecker, W.S., 1982. Glacial to interglacial changes in ocean chemistry. Progress in Oceanography 2, 151–197.

Brzezinski, M.A., Nelson, D.M., Franck, V.M., Sigmon, D.E., 2001. Silicon dynamics within an intense open-ocean diatom bloom in the Pacific sector of the Southern Ocean. Deep-Sea Research II 48, 3997–4018.

Chai, F., Lindley, S.T., Toggweiler, J.R., Barber, R.T., 2000. Testing the importance of iron and grazing in the maintenance of the high nitrate condition in the equatorial Pacific Ocean: a physical-biological model study. In: Hanson, R.B., Ducklow, H.W., Field, J.G. (Eds.), The Changing Ocean Carbon Cycle. Cambridge University Press, Cambridge, pp. 155–185.

Christian, J.R., Verschell, M.A., Murtugudde, R., Busalacchi, A.J., McClain, C.R., 2002a. Biogeochemical modelling of the tropical Pacific Ocean. I. Seasonal and interannual variability. Deep-Sea Research II 49, 509–543.

Christian, J.R., Verschell, M.A., Murtugudde, R., Busalacchi, A.J., McClain, C.R., 2002b. Biogeochemical modelling of the tropical Pacific Ocean. II. Iron biogeochemistry. Deep-Sea Research II 49, 545–565.

Cullen, J.J., 1990. On models of growth and photosynthesis in phytoplankton. Deep-Sea Research I 37, 667–683.

Cullen, J.J., 1991. Hypotheses to explain high-nutrient conditions in the open sea. Limnology and Oceanography 36, 1578–1599.

de Baar, H.J.W., Jong, J.T.M., Bakker, D.C.E., Löscher, B.M., Veth, C., Bathmann, U., Smetacek, V., 1995. Importance of iron for plankton blooms and carbon dioxide drawdown in the Southern Ocean. Nature 373, 412–415.

de Baar, H.J.W., Jong, J.T.M., Nolting, R.F., Timmermans, K.R., van Leeuwe, M.A., Bathmann, U., van der Loff, M.R., Sildam, J., 1999. Low dissolved Fe and absence of diatom blooms in remote Pacific waters of the Southern Ocean. Marine Chemistry 66, 1–34.

Denman, K.L., Peña, M.A., 1999. A coupled 1-D biological physical model of the Northeast Subarctic Pacific Ocean with iron limitation. Deep-Sea Research II 46, 2877–2908.

Dugdale, R.C., Wilkerson, F.P., Minas, H.J., 1995. The role of the silica pump in driving new production. Deep-Sea Research I 42, 697–719.

Elderfield, H., Rickaby, R.E.M., 2000. Oceanic Cd/P ratio and nutrient utilization in the glacial Southern Ocean. Nature 405, 305–310.

Fennel, K., Abbott, M.R., Spitz, Y.H., Richman, J.G., Nelson, D.M., 2003. Modeling controls of phytoplankton production in the southwest Pacific sector of the Southern Ocean. Deep-Sea Research II, this issue (PII: S0967-0645(02)00594-5).

François, R., et al., 1997. Contribution of Southern Ocean surface-water stratification to low atmospheric CO_2 concentrations during the last glacial period. Nature 389, 929–935.

Franck, V.M., Brzezinski, M.A., Coale, K., Nelson, D.M., 2000. Iron and silicic acid concentrations regulate Si uptake north and south of the Polar Frontal Zone in the Pacific Sector of the Southern Ocean. Deep-Sea Research II 47, 3315–3338.

Frost, B., 1991. The role of grazing control in nutrient-rich areas of the open ocean sea. Limnology and Oceanography 36, 1616–1630.

Fung, I.Y., Meyn, S.K., Tegen, I., Doney, S.C., John, J.G., Bishop, J.K.B., 2000. Iron supply and demand in the upper ocean. Global Biogeochemical Cycles 14, 281–295.

Geider, R.J., 1999. Complex lesson of iron uptake. Nature 400, 815–816.

Geider, R.J., La Roche, J., 1994. The role of iron in phytoplankton photosynthesis and the potential for iron-limitation of primary productivity in the sea. Photosynthesis Research 39, 275–301.

Gledhill, M., van den Berg, C.M.G., 1995. Measurement of the redox speciation of iron in seawater by catalytic stripping voltammetry. Marine Chemistry 50, 51–61.

Greene, R.M., Geider, R.J., Falkowski, P.G., 1991. Effect of iron limitation on photosynthesis in a marine diatom. Limnology and Oceanography 36, 1772–1782.

Greene, R.M., Geider, R.J., Falkowski, P.G., 1992. Effect of iron limitation on photosynthesis in a marine diatom. Limnology and Oceanography 36, 1772–1782.

Hense, I., Bathmann, U.V., Timmermann, R., 2000. Plankton dynamics in frontal systems of the Southern Ocean. Journal of Marine Systems 27, 235–252.

Hutchins, D.A., Bruland, K.W., 1998. Iron-limited diatom growth and Si:N uptake ratios in a coastal upwelling regime. Nature 393, 561–564.

Hutchins, D.A., DiTullio, G.R., Bruland, K.W., 1993. Iron and regenerated production: evidence for biological iron recycling in two marine environments. Limnology and Oceanography 38, 1242–1255.

Hutchins, D.A., Wand, W.-X., Fisher, N.S., 1995. Copepod grazing and the biogeochemical fate of diatom iron. Limnology and Oceanography 40, 989–994.

Hutchins, D.A., Witter, A.E., Butler, A., Luther, G.W., 1999. Competition among marine phytoplankton for different chelated iron species. Nature 400, 858–861.

Johnson, K.S., Gordon, R.M., Coale, K.H., 1997. What controls dissolved iron concentrations in the world ocean? Marine Chemistry 57, 137–161.

Knox, F., McElroy, M.B., 1984. Changes in atmospheric CO_2: influence of the marine biota at high latitude. Journal of Geophysical Research 89, 4629–4637.

Kumar, N., Anderson, R.F., Mortlock, R.A., Froelich, P.N., Kubik, P., Dittrich-Hannen, B., Suter, M., 1995. Increased biological productivity and export production in the glacial Southern Ocean. Nature 378, 675–680.

Lancelot, C., Hannon, E., Becquevort, S., Veth, C., de Baar, H.J.W., 2000. Modeling phytoplankton blooms and carbon export production in the Southern Ocean: dominant controls by light and iron in the Atlantic sector in Austral spring in 1992. Deep-Sea Research I 47, 1621–1662.

Lefèvre, N., Watson, A.J., 1999. Modeling the geochemical cycle of iron in the oceans and its impact on atmospheric CO_2 concentrations. Global Biogeochemical Cycles 13, 727–736.

Leonard, C.L., McClain, C.R., Murtugudde, R., Hofmann, E.E., Harding, L.W., 1999. An iron-based ecosystem model of the central equatorial Pacific. Journal of Geophysical Research 104, 1325–1341.

Liebig, J., 1855. Principles of agricultural chemistry with special reference to the late researches made in England. In: Pomeroy, L.R. (Ed.), Cycles of Essential Elements–Benchmark Papers in Ecology, Vol. I (1974). Dowden, Hutchinson and Ross Inc., Stroudsbourg, Pennsylvania, pp. 11–28.

Loukos, H., Frost, B., Harrison, D.E., Murray, J.W., 1997. An ecosystem model with iron limitation of primary production in the equatorial Pacific at 140°W. Deep-Sea Research II 44, 2221–2249.

Martin, J., 1990. Glacial–interglacial CO_2 change: the iron hypothesis. Paleoceanography 5, 1–13.

Measures, C.I., Vink, S., 2001. Dissolved Fe in the upper waters of the Pacific sector of the Southern Ocean. Deep-Sea Research I 48, 3913–3941.

Measures, C.I., Yuan, J., Resing, J.A., 1995. Determination of iron in seawater by flow injection analysis using in-line preconcentration and spectrophotometric detection. Marine Chemistry 50, 3–12.

Mitchell, B.G., Brody, E.A., Holm-Hansen, O., McClain, C., Bishop, J., 1991. Light limitation of phytoplankton biomass and macronutrient utilization in the Southern Ocean. Limnology and Oceanography 36, 1662–1677.

Monnin, E., et al., 2001. Atmospheric CO_2 concentrations over the Last Glacial Termination. Science 291, 112–114.

Moore, J.K., Abbott, M.R., Richman, J.G., Nelson, D.M., 2000. The Southern Ocean at the last glacial maximum: a strong sink for atmospheric carbon dioxide. Global Biogeochemical Cycles 14 (1), 455–475.

Moore, J.K., Doney, S.C., Glover, D.M., Fung, I., 2002a. Iron cycling and nutrient limitation patterns in surface waters of the world ocean. Deep-Sea Research II 49, 463–507.

Moore, J.K., Doney, S.C., Kleypas, J.A., Glover, D.M., Fung, I., 2002b. An intermediate complexity marine ecosystem model for the global domain. Deep-Sea Research II 49, 403–462.

Nelson, D.M., Smith, W.O., 1991. Sverdrup revisited: critical depths, maximum chlorophyll levels, and the control of Southern Ocean productivity by the irradiance-mixing regime. Limnology and Oceanography 36, 1650–1661.

Petit, J.R., et al., 1999. Climate and atmospheric history of the past 420,000 years from the Vostok ice core, Antarctica. Nature 399, 429–436.

Petit, J.R., Mounier, L., Jouzel, J., Korotkevich, K.S., Kotlyakov, V.I., Lorius, C., 1990. Paleoclimatological and chronological implications of the vostok ice core. Nature 343, 56–58.

Popova, E.E., Ryabchenko, V.A., Fasham, M.J.R., 2000. Biological pump and vertical mixing in the Southern Ocean: their impact on atmospheric CO_2. Global Biogeochemical Cycles 14, 477–498.

Price, J.F., Weller, R.A., Pinkel, R., 1986. Diurnal cycling: observations and models of the upper ocean response to diurnal heating, cooling, and wind mixing. Journal of Geophysical Research 91, 8411–8427.

Price, N.M., Ahner, B.A., Morel, F.M.M., 1994. The equatorial Pacific Ocean: grazer-controlled phytoplankton populations in an iron-limited system. Limnology and Oceanography 39, 520–534.

Raven, J.A., 1988. The iron and molybdenum use efficiencies of plant growth with different energy, carbon and nitrogen sources. New Phycologist 109, 279–287.

Redfield, A.C., Ketchum, B.H., Richards, F.A., 1963. The influence if organisms on the composition of seawater. In: Hill, M.N. (Ed.), The Sea. Wiley, New York, pp. 26–77.

Rue, E., Bruland, K.W., 1995. Complexiation of iron(III) by natural organic ligands in the central North Pacific determined by a new competitive equilibration/absorptive cathodic stripping voltammetry method. Marine Chemistry 50, 117–138.

Sarmiento, J.L., Orr, J.C., 1991. Three-dimensional simulations of the impact of Southern Ocean nutrient depletion on atmospheric CO_2 and ocean chemistry. Limnology and Oceanography 36, 1928–1950.

Sarmiento, J.L., Hughes, T.M.C., Stouffer, R.J., Manabe, S., 1998. Simulated response of the ocean carbon cycle to antropogenic climate warming. Nature 393, 245–252.

Scharek, R., van Leeuwe, M.A., de Baar, H.J.W., 1997. Responses of Southern Ocean phytoplankton to the addition of trace metals. Deep-Sea Research II 44, 27–209.

Schmidt, M.A., Zhang, Y., Hutchins, D.A., 1999. Assimilation of Fe and carbon by marine copepods from Fe-limited and Fe-replete diatom prey. Journal of Plankton Research 21, 1753–1764.

Sedwick, P.N., DiTullio, G.R., 1997. Regulation of algal blooms in Antarctic shelf waters by the release of iron from melting sea ice. Geophysical Research Letters 24 (20), 2515–2518.

Sedwick, P.N., DiTullio, G.R., Mackey, D., 1996. Dissolved iron and manganese in surface waters of the Ross Sea, austral summer 1995–96. Antarctic Journal of the US 31, 128–130.

Sedwick, P.N., Edwards, P.R., Mackey, D.J., Griffiths, B.F., Parslow, J.S., 1997. Iron and manganese in surface waters of the Australian subantarctic region. Deep-Sea Research I 44, 1239–1253.

Sigman, D.M., Boyle, E.A., 2000. Glacial/interglacial variations in atmospheric carbon dioxide. Nature 407, 859–869.

Stephens, B., Keeling, R.F., 2000. The influence of Antarctic sea ice on glacial-interglacial CO_2 variations. Nature 404, 171–174.

Sunda, W.G., 1997. Control of dissolved iron concentrations in the world ocean: a comment. Marine Chemistry 57, 169–172.

Sunda, W.G., Huntsman, S.A., 1995. Iron uptake and growth limitation in oceanic and coastal phytoplankton. Marine Chemistry 50, 189–206.

Takeda, S., 1998. Influence of iron availability on nutrient consumption ratio of diatoms in oceanic waters. Nature 393, 774–777.

Toggweiler, J.R., 1999. Variation of atmospheric CO_2 by ventilation of the oceans deepest water. Paleoceanography 14, 571–588.

Wells, M.L., Price, N.M., Bruland, K.W., 1995. Iron chemistry in seawater and its relationship to phytoplankton: a workshop report. Marine Chemistry 48, 157–182.

Wu, J., Luther, G.W., 1995. Complexation if iron(III) by natural organic ligands in the Northwest Atlantic Ocean by a competitive ligand equilibration method and a kinetic approach. Marine Chemistry 50, 159–177.